Global Journal of Pure and Applied Mathematics.
ISSN 0973-1768 Volume 20, Number 3 (2024), pp. 463-482

https://dx.doi.org/10.37622/GJPAM/20.3.2024.463-482

The Riemann Hypothesis and Exponentially Weighted Dirichlet Series

Darrell Cox[1] **and Pedro Caceres** [2]

[1]*Grayson County College, United States.*
[2]*Universidad Europea de Valencia, Spain.*

Abstract

The angles of polar coordinates of a function involving the Riemann zeta function (defined in the critical strip) are used to analyze properties of zeta function zeros. An exponentially weighted Dirichlet series is used to derive a quadratic curve characterizing zeta function zeros.

Keywrods: Riemann zeta function, Riemann hypothesis

1. INTRODUCTION

The Riemann zeta function $\zeta(s)$ for $0 < Re(s) < 1$ can be computed from the η function;

$$\eta(s) = \sum_{n=1}^{\infty} \frac{(-1)^{n+1}}{n^s} = (1 - 2^{1-s})\zeta(s) \tag{1}$$

A plot of the real components of $\zeta(s)$ for the first non-trivial zeta functon zero ($s = (0.5, 14.1347251417)$) and $n \leq 200$ is

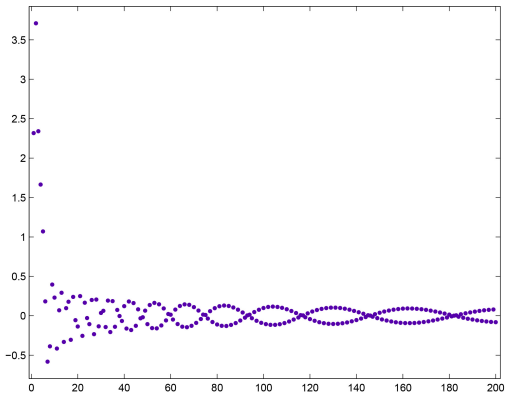

Figure 1

A plot of the values from $n = 147$ to 184 where successive values are connected is

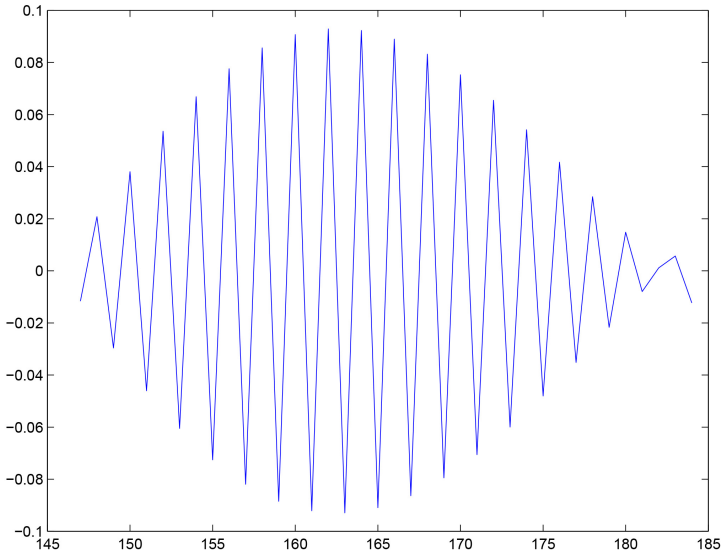

Figure 2

A plot of the n values of the inflection points (where the curve crosses the x-axis from above) for $n \leq 200$ is

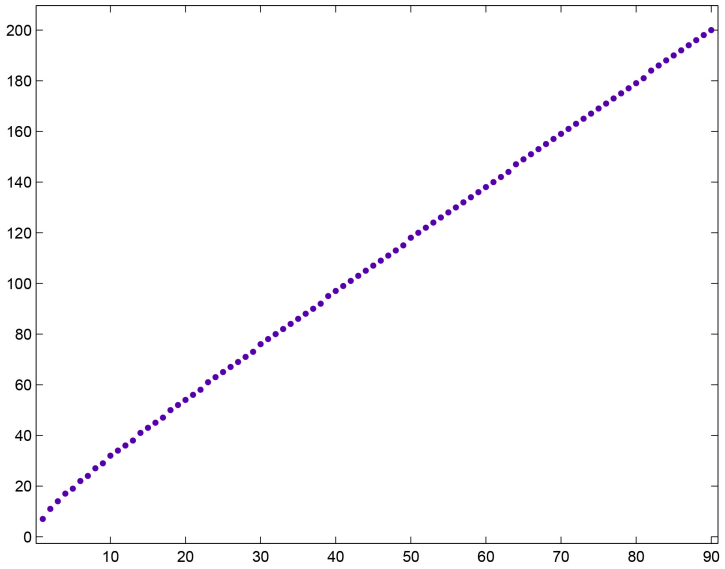

Figure 3

The n values of the inflection points for $n \leq 95$ are 7, 11, 14, 17, 19, 22, 24, 27, 29, 32, 34, 36, 38, 41, 43, 45, 47, 50, 52, 54, 56, 58, 61, 63, 65, 67, 69, 71, 73, 76, 78, 80, 82,

84, 86, 88, 90, 92, and 95. The n values that are at least three greater than the previous n values are 11, 14, 17, 22, 27, 32, 41, 50, 61, 76, and 95. Except for 11, the n values are three greater than the previous n value. The number of n values between 76 and 95 for example is $\frac{95-76-3}{2}$. A plot of the logarithms of the n values that are at least three greater than the previous n values for $n \leq 100000$ is

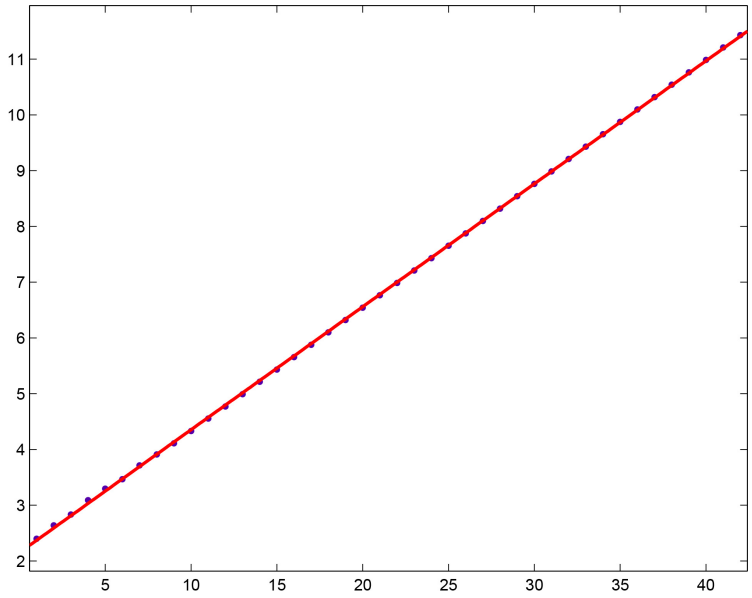

Figure 4

For a linear least-squares fit of the curve, $p_1 = 0.2205$ with a 95% confidence interval of (0.22, 0.2211), $p_2 = 2.15$ with a 95% confidence interval of (2.136, 2.163), SSE=0.01785, R-squared=0.9999, and RMSE=0.02113.

2. A FUNCTION INVOLVING THE RIEMANN ZETA FUNCTION

Let $C(n,a,b)$ denote

$$\frac{2 \cdot n^{-a}}{1-2^{1-s}} \cdot \left(\sum_{j=1}^{n-1} \frac{(-1)^{j+1}}{j^s} \cdot \cos(b \cdot (\ln(\frac{n}{j})))\right) \tag{2}$$

where $s = (a,b)$. See the Methods section for the C code. In polar coordinates, $r = \sqrt{x^2+y^2}$ and θ =atan2(y,x). Cox and Caceres [1] give details on the $C(n,a,b)$ function and polar coordinates.

3. EXPONENTIALLY WEIGHTED DIRICHLET SERIES

A Dirichlet series with exponential terms is

$$D(s) = \sum_{k=1}^{\infty} e^{-ks} \tag{3}$$

where $s = (a, b)$. For $\Re(s) > 0$, the series converges to $e^{-s}/(1 - e^{-s})$. The real part can be expressed as $\sum_{k=1}^{\infty} e^{-ka} \cos(kb)$ and the imaginary part can be expressed as $\sum_{k=1}^{\infty} e^{-ka} \sin(kb)$.

In the first example, the $C(n, a, b)$ function is computed for j values of inflection points (where the curve crosses the x-axis from above) that are at least three greater than the previous j value, $n = 200001$, and $s = (0.0001, 14.1347251417)$. A plot of the logarithms of the j values of the inflection points is

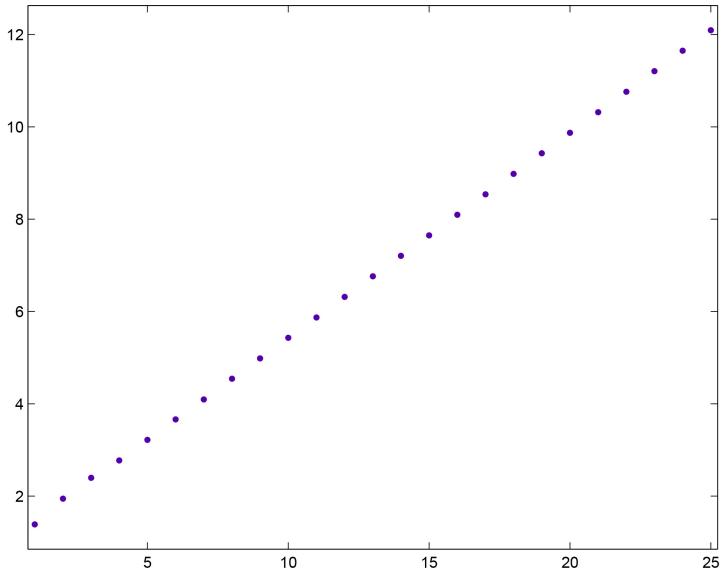

Figure 5

For a linear least-squares fit of the curve (disregarding the first three points), $p_1 = 0.444$ with a 95% confidence interval of (0.4438, 0.443),$p_2 = 0.9918$ with a 95% confidence interval of (0.9879, 0.9957), SSE=0.0002474, R-squared=1, and RMSE=0.003517.

A plot of the corresponding θ values versus the logarithms of the j values of the inflection points is

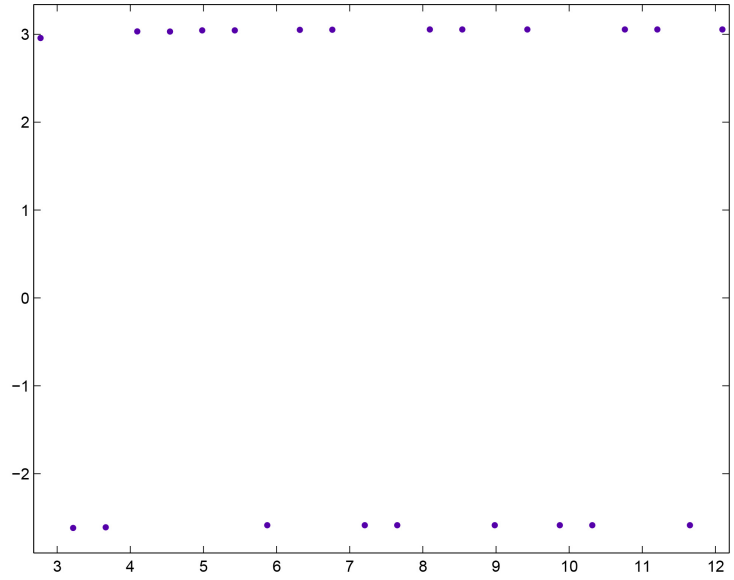

Figure 6

In this instance, the first three θ values are not included. The two curves correspond to even and odd j values.

A plot of the real and imaginary parts of the exponentially weighted Dirichlet series (evaluated at the twenty-five j values of the first graph) versus the logarithms of the j values of the inflection points is

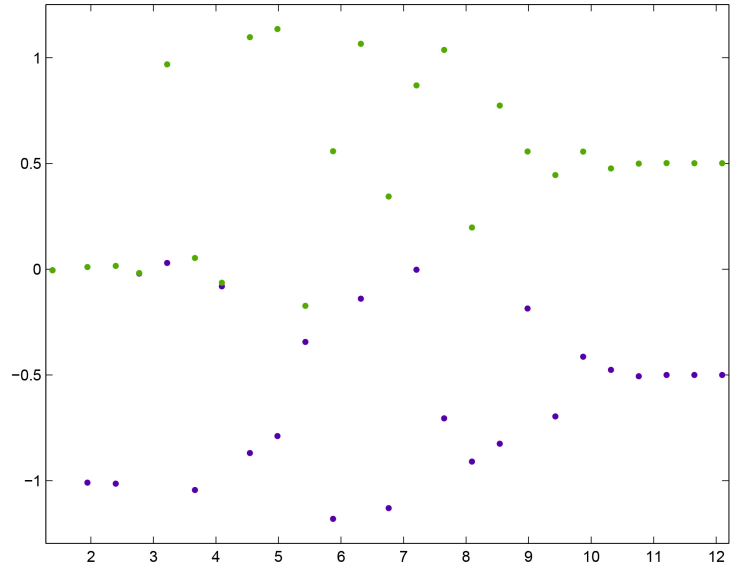

Figure 7

This exponentially weighted Dirichlet series will be denoted by $D(n,a,b)$ to distinguish it from the D series. The series converges to $(-0.499950,\ 0.501222)$. The a value of 0.0001 and n value of 200001 were chosen so that $D(n,a,b)$ converges (slowly) for imaginary parts of the Riemann zeta function zeros. For most imaginary parts of zeta function zeros, the value that the real part of $D(n,a,b)$ converges to is close to -0.4999.

4. EXAMPLE #2

In this example, the $C(n,a,b)$ function is computed for j values of inflection points that are at least three greater than the previous j value, $n = 200001$, and $s = (0.0001, 182.20707848436646)$ (a zeta function zero when $\Re(s) = 0.50$). A plot of the logarithms of the j values of the inflection points is

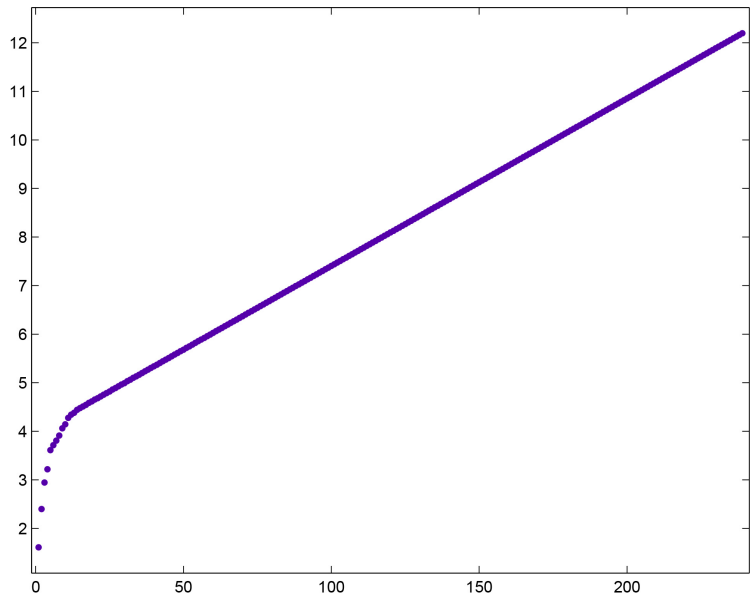

Figure 8

For a linear least-squares fit of the curve (disregarding the first fourteen points), $p_1 = 0.03447$ with a 95% confidence interval of (0.03447, 0.03447), $p_2 = 3.959$ with a 95% confidence interval of (3.958, 3.959), SSE=0.0002934, R-squared=1, and RMSE=0.001144.

A plot of the corresponding θ values versus the logarithms of the j values of the inflection points is

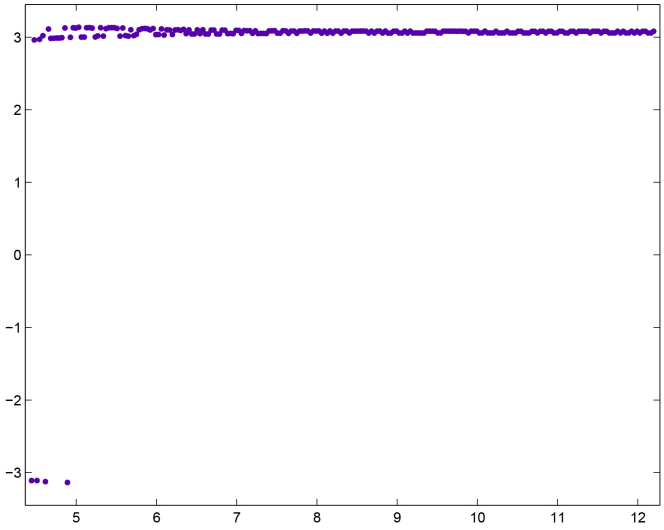

Figure 9

In this instance, the first fourteen θ values are not included.

A plot of the real and imaginary parts of $D(n,a,b)$ (evaluated at the 239 j values in the above graph) versus the logarithms of the j values of the inflection points is

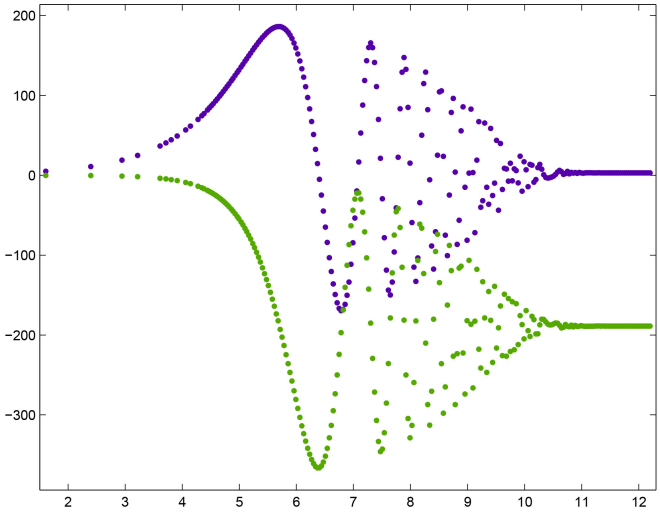

Figure 10

The $D(n,a,b)$ values converge to $(3.064879, -188.774535)$.

A plot of the imaginary parts of $D(n,a,b)$ versus the real parts is

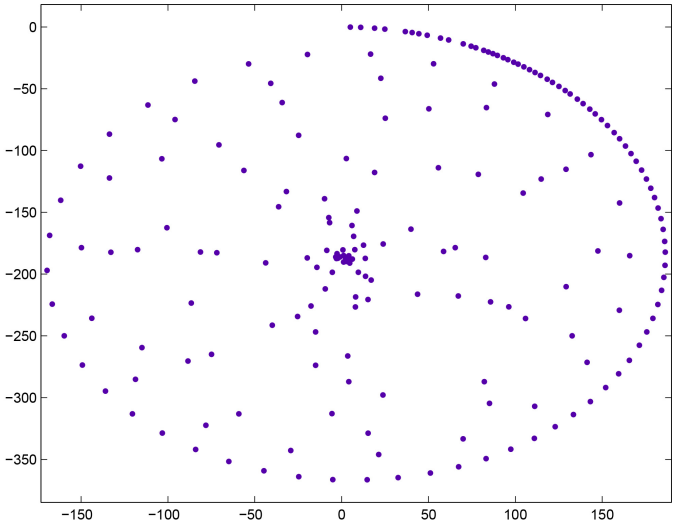

Figure 11

The spiral rotates clockwise starting at a point close to (0,0) and the spiral is centered horizontally on 0.

5. EXAMPLE #3

In this example, the $C(n,a,b)$ function is computed for j values of inflection points that are at least three greater than the previous j value, $n = 200001$, and $s = (0.0001, 276.45204950313291)$ (a zeta function zero when $\Re s) = 0.50$). A plot of the logarithms of the j values of the inflection points is

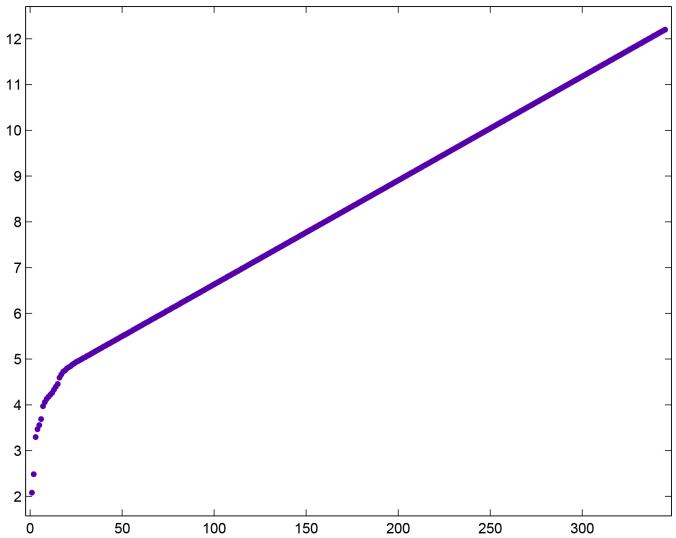

Figure 12

For a linear least-squares fit of the curve (disregarding the first twenty-four points), $p_1 = 0.02272$ with a 95% confidence interval of (0.02272, 0.02272), $p_2 = 4.361$ with a 95% confidence interval of (4.361, 4.361), SSE=0.0002083, R-squared=1, and RMSE=0.0008081.

A plot of the corresponding θ values versus the logarithms of the j values of the inflection points is

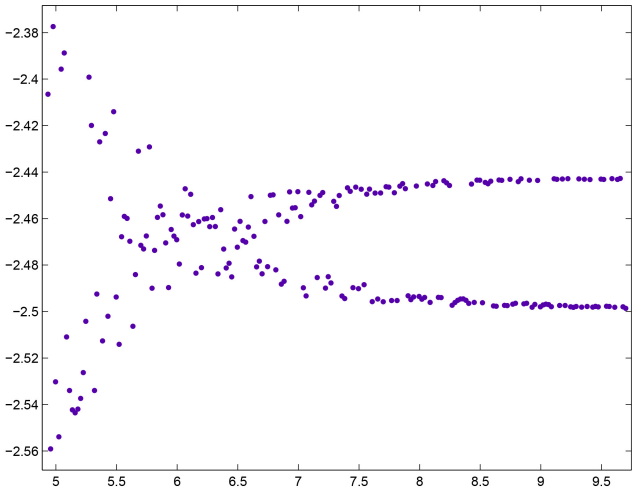

Figure 13

In this instance, the first twenty-four θ values are not included.

A plot of the real and imaginary parts of $D(n,a,b)$ (evaluated at the 345 j values in the above graph) versus the logarithms of the j values of the inflection points is

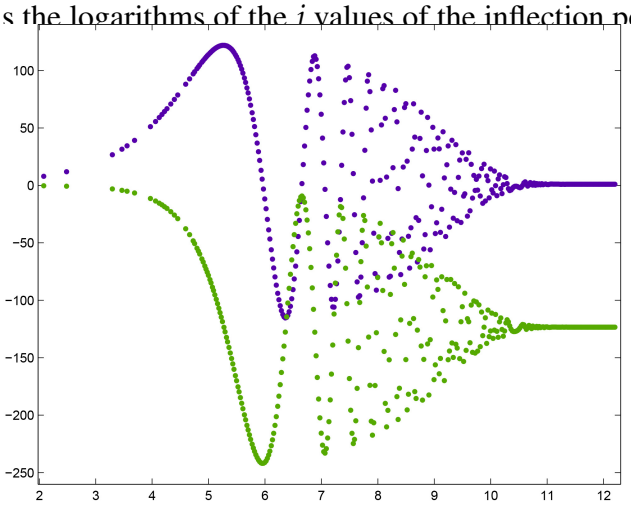

Figure 14

The $D(n,a,b)$ values converge to $(1.022425, -123.376198)$.

A plot of the imaginary parts of $D(n,a,b)$ versus the real parts is

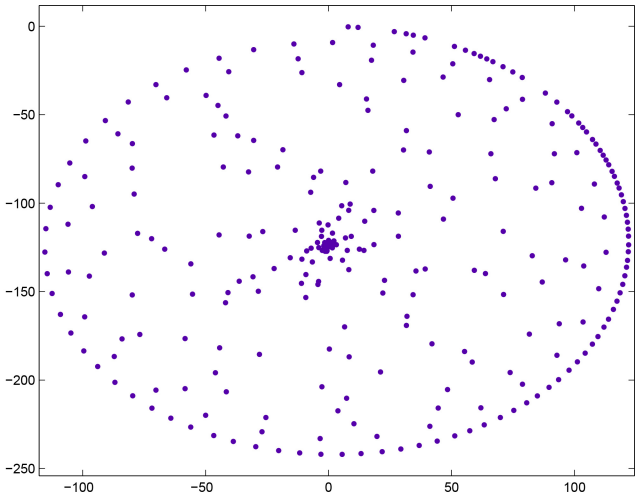

Figure 15

The spiral rotates clockwise starting at a point close to (0,0) and the spiral is centered horizontally on 0.

6. EXAMPLE #4

In this example, the $C(n,a,b)$ function is computed for j values of inflection points that are at least three greater than the previous j value, $n = 200001$, and $s = (0.0001, 351.87864902535927)$ (a zeta function zero when $\Re(s) = 0.50$). A plot of the logarithms of the j values of the inflection points is

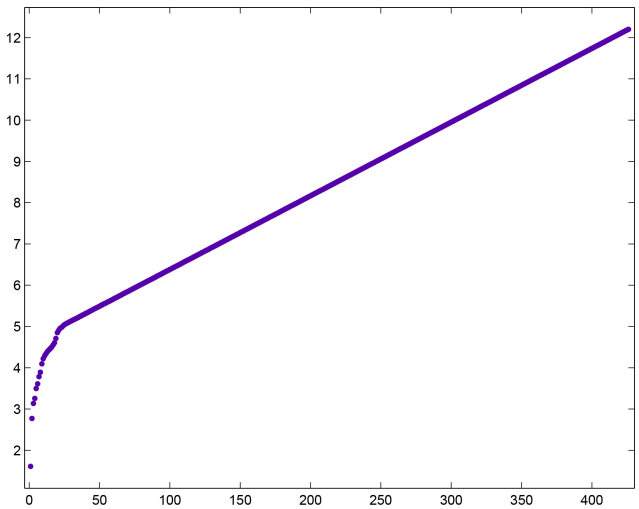

Figure 16

For a linear least-squares fit of the curve (excluding the first twenty-five points), $p_1 = 0.01785$ with a 95% confidence interval of (0.01785, 0.01785), $p_2 = 4.597$ with a 95% confidence interval of (4.596, 4.597), SSE=0.0002338, R-squared=1, and RMSE=0.0007654.

A plot of the corresponding θ values versus the logarithms of the j values of the inflection points is

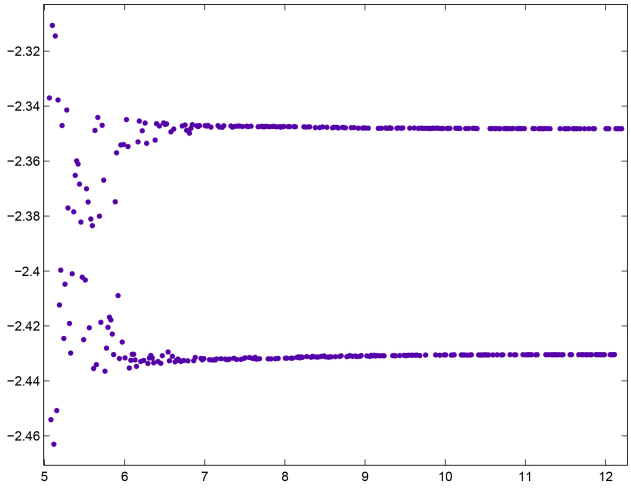

Figure 17

In this instance, the first twenty-five θ values are not included.

A plot of the real and imaginary parts of $D(n,a,b)$ (evaluated at the 426 j values in the above graph) versus the logarithms of the j values of the inflection points is

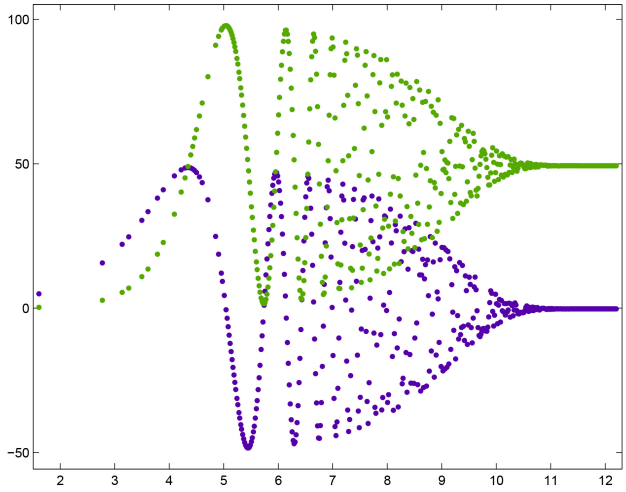

Figure 18

The $D(n,a,b)$ values converge to (0.256657, 49.326664).

A plot of the imaginary parts of $D(n,a,b)$ versus the real parts is

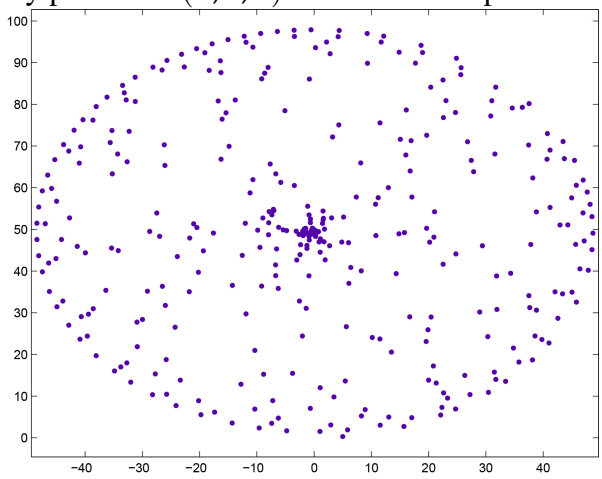

Figure 19

The spiral starts at a point close to (0,0) and rotates counter-clockwise. The spiral is centered horizontally at 0.

7. EXAMPLE #5

In this example, the $C(n,a,b)$ function is computed for j values of inflection points that are at least three greater than the previous j value, $n = 200001$, and $s = (0.0001, 20.0)$ (not a zeta function zero when $\Re(s) = 0.50$). A plot of the logarithms of the j values of the inflection points is

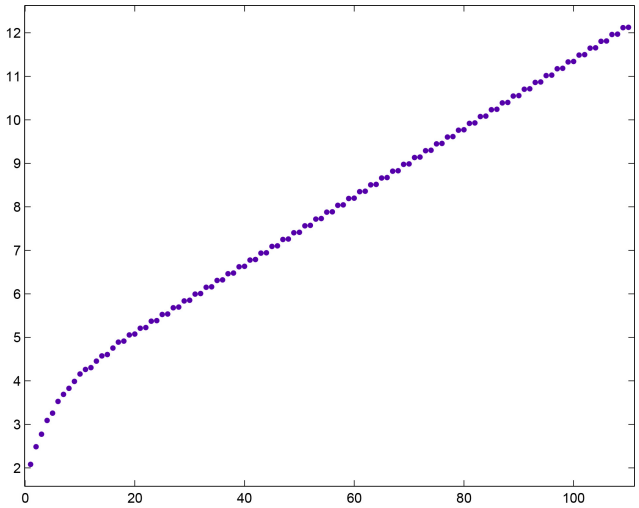

Figure 20

After the first sixteen values, the difference between the j value of an inflection point

and the j value of the previous inflection point is three for every other pair of j values. This accounts for the two separate curves.
A plot of the real and imaginary parts of $D(n,a,b)$ versus the logarithms of the j values of the inflection points is

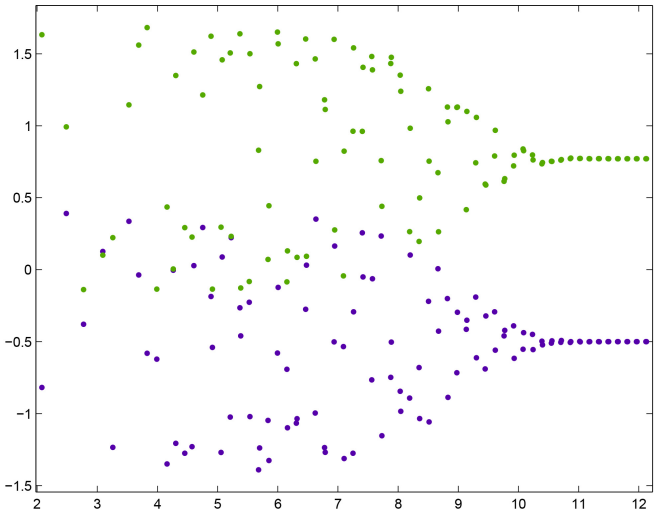

Figure 21

The $D(n,a,b)$ values converge to $(-0.49916, 0.771176)$.

A plot of the imaginary parts of $D(n,a,b)$ versus the real parts is

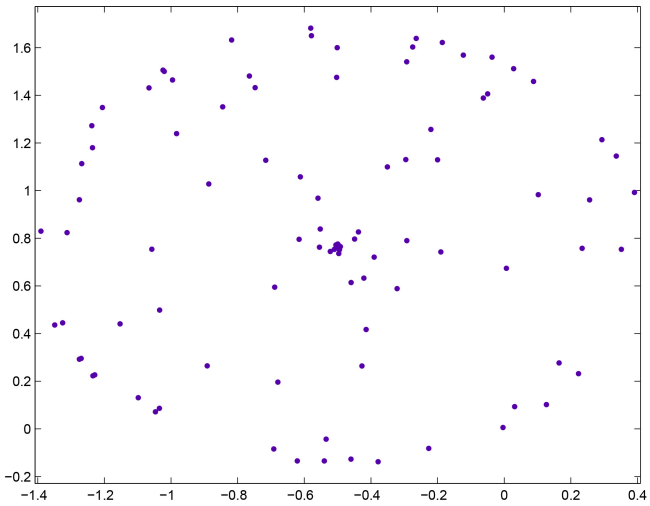

Figure 22

The spiral is not centered horizontally on 0. This appears to occur only for the imaginary parts of zeta function zeros.

8. CONCLUSION

For the zeta function zeros less than 500, there are twenty-six instances where $3.0< |\Im D(n,a,b)| <50.0$. A table of the imaginary parts of the zeta function zeros and the real and imaginary parts of the convergents of $D(n,a,b)$ is

37.58617815882568, -0.4921510383, -8.8453340003,
56.44624769706339, -0.4904586980, -9.7551657891,
75.70469069908393, -0.4989269209, 3.2374145803,
138.11604205453344, -0.4923016942, -8.7597486155,
150.92525761224147, -0.4939647108, 7.7526161131,
169.91197647941169, -0.4985780576, 3.7375863692,
201.26475194370380, -0.4975607411, 4.9135141879,
213.34791935971268, -0.4987195847, -3.5431782001,
251.01494779501601, -0.4989673902, -3.1742821314,
263.57389390487015, -0.4990143853, -3.0993810892,
282.46511476505208, -0.4986997987, -3.5710097167,
295.57325487895827, -0.4985518716, 3.7724239251,
301.64932546219416, -0.4685889455, 17.7160865159,
313.98528573115891, -0.4966879239, -5.7332918860,
351.87864902535927, -0.2566570369, 49.3266642910,
357.95268510163226, -0.4971885555, -5.2786888150,
364.73602411408899, -0.4989595661, 3.1865979632,
383.44352944953647, -0.4964997234, 5.8951565776,
395.58287001099370, -0.4984870504, -3.8574025199,
401.83922860053320, -0.4987572978, -3.4895682466,
415.01880975515513, -0.4990653895, 3.0159723734,
420.64382762504181, -0.4990710456, -3.0065756491,
427.20882508407459, -0.4561807362, -20.9270240074,
439.91844221437066, -0.4890203174, 10.4664479011,
483.85142721248252, -0.4530570339, 21.6605058467,
496.42969621575912, -0.4703235439, 17.2195776767,

A plot of the real parts of $D(n,a,b)$ versus the absolute values of the imaginary parts is

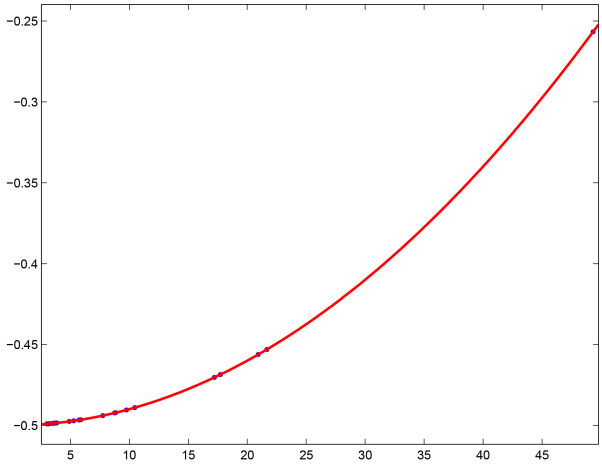

Figure 23

For a quadratic least-squares fit of the curve, $p_1 = 0.0001$ with a 95% confidence interval of (0.0001, 0.0001), $p_2 = -7.861 \cdot 10^{-8}$ with a 95% confidence interval of $(-8.878 \cdot 10^{-8}, -6.884 \cdot 10^{-8})$, $p_3 = -.5$ with a 95% confidence interval of $(-.5, -.5)$, SSE=$1.507 \cdot 10^{-13}$, R-squared=1, and RMSE=$8.095 \cdot 10^{-8}$. This result can be extended to include absolute values of $\Im D(n,a,b)$ less than 3.0 and greater than 50.0.

A plot of the convergents of the real parts of $D(n,a,b)$ versus the imaginary parts for the first five thousand zeta function zeros is

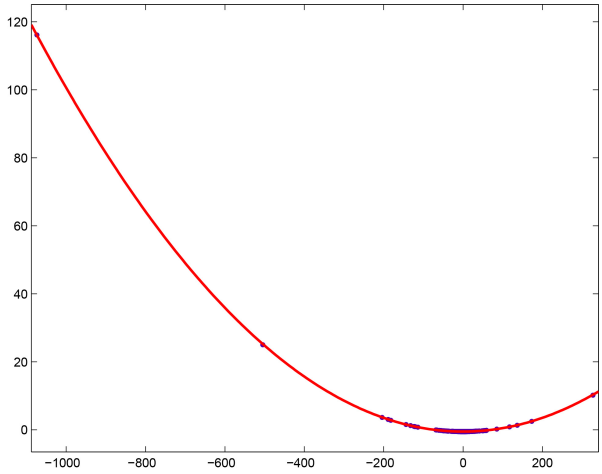

Figure 24

For a quadratic least-squares fit of the curve, $p_1 = 0.0001012$ with a 95% confidence

interval of (0.0001012, 0.0001012), $p_2 = 4.789 \cdot 10^{-5}$ with a 95% confidence interval of $(3.832 \cdot 10^{-5}, 5.747 \cdot 10^{-5})$, $p_3 = -0.5001$ with a 95% confidence interval of $(-0.5002, -0.50)$, SSE=0.07198, R-squared=1, and RMSE=0.003795. The curve resembles a parabola. Caceres [2] gives a theoretical explanation for this.

A plot of the real parts of the convergents of $D(n,a,b)$ versus the imaginary parts for $n = 3000001$, $a = 0.00005$, and the first ten thousand zeta function zeros is

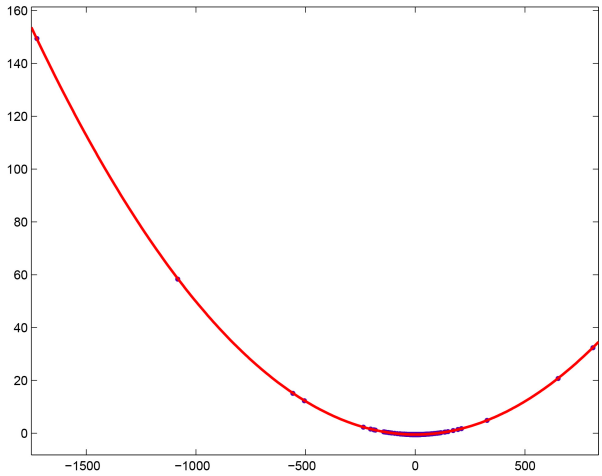

Figure 25

For a quadratic least-squares fit of the curve, $p_1 = 5.03 \cdot 10^{-5}$ with a 95% confidence interval of $(5.03 \cdot 10^{-5}, 5.03 \cdot 10^{-5})$, $p_2 = -4.499 \cdot 10^{-5}$ with a 95% confidence interval of $(-4.851 \cdot 10^{-5}, -4.147 \cdot 10^{-5})$, $p_3 = -0.5001$ with a 95% confidence interval of $(-.5001, -.5001)$, SSE=0.1157, R-squared=1.0, and RMSE=0.003401.

9. METHODS

```
    #include <math.h>
#include <stdio.h>
//
// compute C(n,a,b), 09/20/2024 (dkc)
//
unsigned int max=2001;
double a=0.51;
//double b=14.13472514173470;
double b=21.02203963877156;
```

```
//double b=25.01085758014569;
//double b=30.42487612585951;
//double b=32.93506158773919;
//double b=37.58617815882568;
//double b=40.91871901214750;
//double b=43.32707328091500;
//double b=48.00515088116716;
//double b=49.77383247767230;
//double b=52.97032147771446;
//double b=56.44624769706339;
//double b=59.34704400260235;
//double b=60.83177852460981;
//double b=65.11254404808160;
//double b=67.07981052949417;
//double b=69.54640171117399;
//double b=72.06715767448191;
//double b=75.70469069908393;
//double b=77.14484006887480;
//double b=79.33737502024937;
//double b=84.73549298051705;
//double b=87.42527461312523;
//double b=88.80911120763446;
//double b=92.49189927055849;
//double b=94.65134404051989;
//double b=95.87063422824531;
//double b=98.83119421819369;
//double b=101.31785100573138;
unsigned int xmin=0; // usually set to 0
unsigned int out=2; // usually 1, 2 for inflection points
unsigned int out3p=1; // usually 0, 1 for differences in j values >=2
unsigned int polar=1; // set to use polar coordinates
void main() {
unsigned int x,oldx;
double sumr,sumi,R,I,temp1,oldsumr,oldsumi,temp,tempa,tempb,y,e,f,g;
double tempr,esumr,esumi;
FILE *Outfp;
Outfp = fopen("c2nab2f.dat","w");
y=1.0-a;
```

```
if (y>=0.0)
    temp1=pow((double)2,y);
else {
    temp1=pow((double)2,-y);
    temp1=1.0/temp1;
    }
e=temp1*(cos(b*log(2)));
f=temp1*(sin(b*log(2)));
e=1.0-e;
f=-f;
y=-a;
if (y>=0.0)
    temp1=pow((double)max,y);
else {
    temp1=pow((double)max,-y);
    temp1=1.0/temp1;
    }
y=2.0*temp1;
oldx=0;
sumr=0.0;
sumi=0.0;
oldsumi=0.0;
oldsumr=0.0;
esumr=0.0;
esumi=0.0;
for (x=1; x<=(max-1); x++) {
    tempr=1.0/exp((double)x*a);
    esumr=esumr+tempr*cos((double)x*b);
    esumi=esumi+tempr*sin((double)x*b);
    temp1=pow((double)x,a);
    R=temp1*cos(b*log((double)x));
    I=temp1*sin(b*log((double)x));
    temp1=R*R+I*I;
    if (x!=(x/2)*2) {
        sumr=sumr+R/temp1;
        sumi=sumi-I/temp1;
        }
    else {
```

```
        sumr=sumr-R/temp1;
        sumi=sumi+I/temp1;
        }
    temp=cos(b*log((double)max/(double)x));
    tempa=sumr*temp;
    tempb=sumi*temp;
    tempa=tempa*y;
    tempb=tempb*y;
    g=tempa*e-tempb*f;
    tempb=tempa*f+tempb*e;
    tempa=g;
    if (x>xmin) {
        if (out==1)
            fprintf(Outfp," %.10llf, %.10llf \n",tempa,tempb);
        if ((out==2)&&((oldsumr¿0.0)&&(tempa¡0.0))) {
            if (out3p==0)
                fprintf(Outfp," %d %.10llf %.10llf \n",x,tempa,tempb);
            if ((x-oldx)>2) {
                printf(" %d %d %.10llf %.10llf \n",x,oldx,oldsumr,tempa);
                if (out3p!=0) {
                    if (polar==0)
                        fprintf(Outfp," %d %d \n",x,oldx);
                    else
                        fprintf(Outfp," %d %d %.10llf %.10llf %.10llf %.10llf
\n",x,oldx,
                            sqrt(tempa*tempa+tempb*tempb),atan2(tempb,tempa),esumr,esumi);
                    }
                }
            oldx=x;
            }
        oldsumr=tempa;
        oldsumi=tempb;
        }
    }
fclose(Outfp);
return;
}
```

REFERENCES

[1] Cox, D. and Caceres, P., The Riemann Hypothesis and Polar Coordinates, *Global Journal of Pure and Applied Mathematics*, ISSN 0973-1768 Volume 20, Number 3 (2024), pp. 432-462, @Research India Publications

[2] Caceres, P., Ellipse Symmetry in Dirichlet Series: A Duality Between Analytic (Riemann Zeta) and Geometric Forms, DOI 10.13140/RG.2.2.17565.52960